

Original research

Serum glucose excretion after Roux-en-Y gastric bypass: a potential target for diabetes treatment

In Gyu Kwon ¹, Chan Woo Kang ², Jong-Pil Park ³, Ju Hun Oh ^{2,4}, Eun Kyung Wang ⁴, Tae Young Kim ⁵, Jin Sol Sung ², Namhee Park ⁶, Yang Jong Lee ⁴, Hak-Joon Sung ⁵, Eun Jig Lee ⁴, Woo Jin Hyung ⁷, Su-Jin Shin ⁸, Sung Hoon Noh ¹, Mijin Yun ⁶, Won Jun Kang ⁶, Arthur Cho ⁶, Cheol Ryong Ku ⁴

► Additional material is published online only. To view please visit the journal online (<http://dx.doi.org/10.1136/gutjnl-2020-321402>).

For numbered affiliations see end of article.

Correspondence to

Dr Cheol Ryong Ku, Endocrinology, Institute of Endocrine Research, Department of Internal Medicine, Yonsei University College of Medicine, Seoul, Republic of Korea; cr079@yuhs.ac and Dr Arthur Cho, Department of Nuclear Medicine, Yonsei University College of Medicine, Seoul, Republic of Korea; artycho@yuhs.ac

IGK and CWK contributed equally.

Received 13 April 2020
Revised 4 November 2020
Accepted 5 November 2020



© Author(s) (or their employer(s)) 2020. No commercial re-use. See rights and permissions. Published by BMJ.

To cite: Kwon IG, Kang CW, Park J-P, et al. *Gut* Epub ahead of print: [please include Day Month Year]. doi:10.1136/gutjnl-2020-321402

ABSTRACT

Objective The mechanisms underlying type 2 diabetes resolution after Roux-en-Y gastric bypass (RYGB) are unclear. We suspected that glucose excretion may occur in the small bowel based on observations in humans. The aim of this study was to evaluate the mechanisms underlying serum glucose excretion in the small intestine and its contribution to glucose homeostasis after bariatric surgery.

Design 2-Deoxy-2-[¹⁸F]-fluoro-D-glucose (FDG) was measured in RYGB-operated or sham-operated obese diabetic rats. Altered glucose metabolism was targeted and RNA sequencing was performed in areas of high or low FDG uptake in the ileum or common limb. Intestinal glucose metabolism and excretion were confirmed using ¹⁴C-glucose and FDG. Increased glucose metabolism was evaluated in IEC-18 cells and mouse intestinal organoids. Obese or *ob/ob* mice were treated with amphiregulin (AREG) to correlate intestinal glycolysis changes with changes in serum glucose homeostasis.

Results The AREG/EGFR/mTOR/AKT/GLUT1 signal transduction pathway was activated in areas of increased glycolysis and intestinal glucose excretion in RYGB-operated rats. Intraluminal GLUT1 inhibitor administration offset improved glucose homeostasis in RYGB-operated rats. AREG-induced signal transduction pathway was confirmed using IEC-18 cells and mouse organoids, resulting in a greater capacity for glucose uptake via GLUT1 overexpression and sequestration in apical and basolateral membranes. Systemic and local AREG administration increased GLUT1 expression and small intestinal membrane translocation and prevented hyperglycaemic exacerbation.

Conclusion Bariatric surgery or AREG administration induces apical and basolateral membrane GLUT1 expression in the small intestinal enterocytes, resulting in increased serum glucose excretion in the gut lumen. Our findings suggest a novel, potentially targetable glucose homeostatic mechanism in the small intestine.

INTRODUCTION

Since the serendipitous finding that type 2 diabetes is improved through Roux-en-Y gastric bypass (RYGB) more than three decades ago,^{1,2} multicentre trials have revealed that gastric bypass is the most effective method to treat type 2 diabetes mellitus in

Significance of this study

What is already known on this subject?

- Patients with type 2 diabetes experience a rapid improvement in serum glucose within months of Roux-en-Y gastric bypass (RYGB).
- Known mechanisms for serum glucose improvement after gastric bypass have been attributed to anatomical, gut physiological and endocrinological changes.
- In rodent models, intestinal hypertrophy and increased glycolysis have been shown in the common limb (CL) as well as alimentary limb after RYGB.
- Changes in intestinal glycolysis after gastrectomy have been identified using ¹⁸F-fluoro-2-deoxyglucose (FDG) positron emission tomography/CT (PET/CT), which were reported to be correlated with weight loss and improvement in serum glucose levels.

obese patients.^{3,4} However, the mechanisms underlying the rapid resolution of serum glucose levels after bariatric surgery remain unclear, and a pharmacological agent that can mimic this effect has not yet been identified.

¹⁸F-fluoro-2-deoxyglucose (FDG) positron emission tomography/CT (PET/CT) in post-gastrectomy patients shows changes in intestinal glycolysis, which are associated with a reduction in the serum glucose level⁵ and weight loss.⁶ Furthermore, we clinically observed that small intestine glycolysis migrates, as revealed by repeated PET/CT scans performed on the same day. Based on these findings, we hypothesised that serum glucose may be excreted into the small intestine, which might contribute to the rapid improvement of glucose homeostasis after bariatric surgery.

To test this hypothesis, we first evaluated whether serum glucose is excreted into the intestinal lumen after RYGB in an obese, diabetic rat model. We then targeted areas of increased glycolysis in the intestine and evaluated the activated signalling pathways in comparison with areas of low glycolysis and sham-operated intestine. Lastly, we mimicked the glucose-excretion effect of RYGB by pharmaceutical administration of amphiregulin (AREG),

Significance of this study

What are the new findings?

- ▶ mRNA analysis of areas of increased glycolysis in the CL showed glucose transporter 1 (GLUT1) and amphiregulin (AREG) overexpression in RYGB rats.
- ▶ Intravenously injected FDG and ¹⁴C-glucose were detected in the lumen of the CL in RYGB rats, which suggests that serum glucose is excreted into the intestinal lumen after RYGB.
- ▶ The AREG/EGFR/mTOR/AKT/GLUT1 signal transduction pathway was confirmed in intestinal cells, which resulted in GLUT1 overexpression and sequestration in apical and basolateral membranes.
- ▶ Intraluminal GLUT1 inhibitor administration reduced the RYGB-induced effects of glucose homeostasis improvement.
- ▶ Systemic and intraluminal AREG administration mimicked the RYGB-induced glucose-lowering effect in obese and hyperglycaemic mice.
- ▶ Our study shows that serum glucose is excreted into the intestinal lumen after RYGB, and this phenotype is mimicked after AREG administration.

How might it impact on clinical practice in the foreseeable future?

- ▶ Our results suggest that the intestine may be a conduit for serum glucose loss via intestinal glucose excretion, which may be a potential novel target for improving systemic glucose homeostasis.

which was found to be overexpressed after RYGB. We confirmed the contribution of glucose transporter 1 (GLUT1) expression and sequestration in the small intestine by locally administering a GLUT1 inhibitor. In addition, we evaluated whether this effect could be observed in post-RYGB human specimens as well as in a small cohort of clinical post-gastrectomy diabetic patients and investigated the association between improvement in the HbA1c level and FDG uptake in the small intestine.

MATERIALS AND METHODS

Detailed descriptions are provided in the Supplemental Methods.

All animal experiments and animal care were performed in accordance with the guidelines of and approved by the Institutional Animal Care and Use Committee of the Severance Hospital, Seoul, Republic of Korea (IACUC approval no: 2016-0041).

Establishment of the bariatric surgery animal model

High-fat diet (HFD)-induced obesity (DIO) male Otsuka Long-Evans Tokushima fatty (OLETF) rats underwent either RYGB or sham surgery. The oral glucose tolerance test (OGTT) was performed 1 month after surgery and FDG μ PET was performed the next day after fasting overnight. The μ PET scan was performed 1 hour after intravenous FDG injection. Immediately after μ PET, the rats were sacrificed and the intestines were excised en bloc. The limbs were then flushed with phosphate buffered saline (PBS), and PBS washings were collected for gamma counting to quantify the amount of FDG excreted into the intestinal lumen. Autoradiography images of the post-wash intestines were acquired to identify areas of high glycolytic rates within the intestinal wall. Blood samples were obtained immediately before euthanasia and were evaluated for changes in hormone levels.

To determine glucose excretion into the intestinal lumen as well as the contribution of each limb in serum glucose intestinal excretion, we repeated the RYGB/sham experiments using DIO SD rats with the following two modifications: a mixture of FDG and ¹⁴C-glucose was intravenously injected immediately after ligating each limb at the anastomosis site (illustration in online supplemental figure S1A), and the radioactivity of both FDG and ¹⁴C-glucose in the intraluminal washings 1 hour after injection was measured. Other procedures were similar to those previously described.

This animal model was also used to evaluate the glucose homeostasis effect of GLUT1 inhibition in RYGB-operated OLETF rats. Hydrogel containing either a specific GLUT1 inhibitor (STF-31, 10 mg/kg; Sigma-Aldrich, St. Louis, Missouri, USA) or PBS was implanted in the common limb (CL) during RYGB or sham surgery. Rats were sacrificed 8 days after hydrogel implantation, and a similar protocol was performed as described above.

Total RNA sequencing

Immediately after autoradiography, the images were digitally overlaid with a photograph of the intestinal specimens, and samples of each limb that had either increased or decreased FDG uptake were collected for total RNA sequencing. Corresponding areas of the sham-operated intestine were also used as controls.

Total RNA was isolated using RNeasy Mini Kit (Qiagen, Germantown, Maryland, USA) following the manufacturer's instructions. Total RNA integrity was assessed using an Agilent Technologies 2100 Bioanalyzer based on the RNA integrity number value. Total RNA sequencing libraries were prepared using an Illumina TruSeq Stranded Total RNA Sample prep kit with Ribo-zero Human/Mouse/Rat, following the manufacturer's instructions. After qPCR using SYBR Green PCR Master Mix (Applied Biosystems, Waltham, Massachusetts, USA), libraries were combined such that index-tagged samples were represented in AREG equimolar amounts within the pool.

Cell culture

The IEC-18 cell line was obtained from the Seoul National University Hospital Cell Line Bank (Seoul, Republic of Korea). Cells were treated with AREG or vehicle for 24 hours for gamma count analysis and flow cytometry.

***In vitro* ¹⁴C-glucose uptake assay**

IEC-18 cells were treated with AREG or vehicle for 24 hours before the *in vitro* assays. The cells were then incubated in 0–50 mM glucose spiked with ¹⁴C-glucose (0.5 μ Ci, specific activity: 300 μ Ci/mmol) for 10 min. Cells were then washed, lysed and beta-counted using liquid scintillation analyser.

Crypt isolation and culture for organoid studies

The small intestines of C57BL/6J mice were harvested. The fat and villi were removed and the samples were incubated at 24°C for 15 min to isolate the crypts. After passing the crypt suspension through a cell strainer and centrifugation, 50–200 crypts were suspended in 25 μ L of Matrigel (#356231; BD, Franklin Lakes, New Jersey, USA).

GLUT1 surface staining

To examine surface GLUT1 expression, IEC-18 cells and mouse intestinal organoids were incubated either with AREG (100 ng/mL) or PBS for 1 hour and stained with a fluorochrome (PE)-conjugated GLUT1 antibody (1:50; NB110-39113PE) for 1 hour. Cells were analysed using a FACSVERSE instrument

(BD Biosciences, San Jose, California, USA) and FlowJo (BD Biosciences).

Evaluation of the glucose homeostatic response to pharmaceutically administered AREG in animal models

Four-week-old male DIO C57BL/6J mice were used to evaluate the systemic effects of AREG treatment. The HFD diet was introduced for 20 weeks, mouse recombinant AREG protein or PBS was injected intraperitoneally (100 μ L/day, 4 weeks), and the HFD was continued.

Sixteen-week-old C57B1/6J *lep ob/ob* male mice were used to evaluate localised AREG treatment. Hydrogels containing mouse recombinant AREG or PBS were implanted into the ileal lumen of *ob/ob* mice for 1 week.

In both models, baseline OGTT was performed before AREG treatment, and post-treatment OGTTs were performed before euthanasia. Tissues and blood samples were collected and analysed using ELISA for hormonal changes, and immunohistochemistry (IHC) or western blot analysis was performed to evaluate glycolysis-related signal transduction.

Histology and immunostaining

Intestinal tissues from the animal models were paraffin-embedded and sectioned. Tissue sections (4 μ m thick) were cut from each block for either H&E staining or immunostaining with the following antibodies: mouse anti-AREG, rabbit anti-GLUT1, mouse anti-CD4. For IHC and mouse intestinal organoids, cells cultured on coverslips were washed with ice-cold PBS and fixed in 4% paraformaldehyde. The cells were then incubated with anti-GLUT1 and anti-PEPT-1 antibodies.

Analysis of clinical data of patients with gastrectomy

Medical charts of diabetic patients with gastric cancer who underwent FDG PET/CT at 6–12 months after gastrectomy were reviewed to evaluate relapse. Seventeen patients with tumor, nodes, metastasis (TNM) stage Ia (AJCC seventh edition) gastric cancer without any malignancies detected using postoperative FDG PET/CT, and who had undergone no adjuvant chemotherapy within 3 months before FDG PET/CT were selected. A reduction in serum HbA1c levels ($\geq 1\%$) was correlated with small intestinal FDG uptake on semiquantitative analysis. This study was conducted in accordance with the Declaration of Helsinki and was approved by the institutional review board of our hospital (4-2018-0595).

Statistical analysis

Data from the animal and in vitro studies were analysed using Prism software V.4.0.0 (GraphPad, La Jolla, California, USA). For clinical data, statistical analyses were performed using SPSS V.25.0 for Windows (SPSS, Chicago, Illinois, USA). $P < 0.05$ was considered statistically significant.

RESULTS

Heterogeneous FDG biodistribution changes in the common limb (CL) after RYGB

To determine the effects of RYGB on weight loss and metabolic alterations, RYGB and sham surgery was performed on DIO OLETF rats. Thirty days after surgery, RYGB rats exhibited lower body mass compared with that in sham-operated OLETF rats (-14.7% vs $+10.8\%$, respectively, % reduction compared with preoperative weight). Area under the curve (AUC) comparison of OGTT showed significantly improved glucose tolerance (figure 1A). Absolute body weight

(810.5 ± 107.1 vs 611.8 ± 70.33 g, $p < 0.01$) and serum insulin levels (3.78 ± 1.12 ng/mL vs 1.14 ± 0.70 ng/mL, $p < 0.01$) were also significantly low in the RYGB-operated rats (figure 1B,C). No marked changes were observed in fasting plasma GLP-1 levels (8.17 ± 10.78 pg/mL vs 62.79 ± 56.85 pg/mL, ns, non-significant, figure 1D). These findings were consistent with the systemic improvements in glucose metabolism previously reported in human patients following bariatric surgery, demonstrating model relevance.

To evaluate whether RYGB enhanced intestinal glucose uptake and excretion into the intestinal lumen, we performed baseline and post-surgical FDG μ PET and washed the intestinal lumen to detect excreted FDG. In RYGB rats, FDG uptake in the small intestine was increased after surgery, whereas in sham-operated rats, no difference in FDG uptake was observed (figure 1E and online supplemental movie S1A, preoperative, S1B, post-RYGB). Immediately after μ PET, the GI tract was removed, and each limb was washed with PBS to quantify excreted FDG. The post-lavage fluid in the CL, alimentary limb (AL) and biliopancreatic limbs (BPL) was combined and analysed for radioactivity. There was significantly more FDG excreted in the RYGB-operated rat intestinal lumen compared with that of sham-operated rats (1.65 ± 2.05 vs 0.31 ± 0.11 percent injected dose (ID%), $p = 0.028$) (figure 1F, right bar graph). Multiple organs were also removed and FDG uptake evaluation was performed to evaluate systemic changes in glucose metabolism after RYGB operation. Radiotracer tissue distribution analysis showed that FDG uptake in the liver and muscle was lower in the RYGB-operated rats compared with that in sham-operated rats (figure 1F, left bar graph).

After intraluminal washing, FDG autoradiography was performed in the post-washed small intestine to quantify FDG uptake differences in each limb and to target areas of increased glycolysis for RNA seq analysis. RYGB rats exhibited higher FDG uptake in the CL than that in the sham-operated rats (figure 1G and online supplemental figure S1F). Quantification analysis of these autoradiography images showed significantly higher amounts of FDG in the intestinal tissue of CL and AL compared with that in the corresponding sham intestine, and this difference was higher in the CL compared with that in the AL (figure 1H).

Because FDG is not a substrate for SGLT, we used 14 C-glucose to evaluate glucose excretion in RYGB-operated SD rats. Each limb was separately ligated to quantify the amount of glucose excreted into each limb (online supplemental figure S1A). There were higher amounts of 14 C-glucose excretion in the CL compared with that in the corresponding sham limb (0.730 ± 1.306 ID% vs 0.062 ± 0.013 ID%, $p < 0.05$, $n = 8$ RYGB, $n = 5$ sham, online supplemental figure S1D,E). No difference was observed in intestinal glucose excretion in the AL+BPL compared with that in the corresponding limbs in the sham-operated rats (FDG: 1.393 ± 0.834 vs 1.312 ± 1.035 , 14 C-glucose: 0.717 ± 0.974 vs 0.208 ± 0.125 , online supplemental figure S1D, E).

We obtained similar findings in patients with diabetes who underwent FDG PET/CT 1 year after gastrectomy with the Roux-en-Y anastomosis procedure for gastric cancer. FDG PET/CT revealed a strong correlation between the reduction in HbA1c ($\geq -1\%$ vs $< -1\%$) levels and increased FDG uptake in the small intestine (total glycolysis, TG: 157.2 ± 101.3 vs 63.2 ± 102.3 , $p = 0.006$, online supplemental table S1, figure 1I,J). HbA1c improvement was dependent on intestinal glycolysis, and was independent of weight loss (-8.3 ± 9.8 vs -3.9 ± 2.8 , $p = 0.277$) or body mass index (BMI) changes. Together, these data suggested

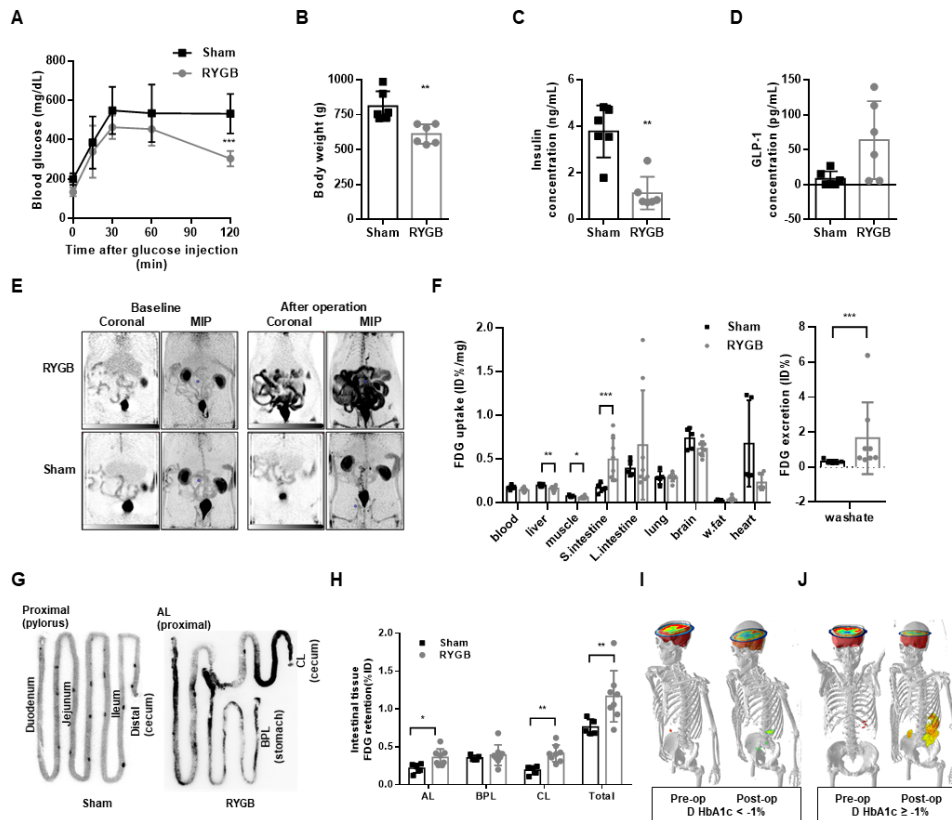


Figure 1 Roux-en-Y gastric bypass (RYGB) leads to sustained weight loss and improves glycaemic control. (A) Oral glucose tolerance test (OGTT) data for sham-operated and RYGB-operated rats. RYGB-operated Otsuka Long-Evans Tokushima fatty (OLETF) rats exhibited better glucose tolerance than sham-operated rats ($n=6$, analysis of variance (ANOVA) two-stage step-up method of Benjamini, Krieger and Yekutieli for multiple comparison correction). (B–D) Mean body mass, fasting serum insulin and glucagon-like peptide-1 concentrations in sham-operated and RYGB-operated rats ($n=6$, unpaired *t*-test). (E) Sequential μ PET images before and after surgery in RYGB-operated or sham-operated rats. Colour bars indicate the range of 0–300 kBq/cc. (F) Left graph: 2-Deoxy-2-[18 F]-fluoro-D-glucose (FDG) biodistribution analysis in RYGB-operated and sham-operated rats revealing higher FDG uptake in the intestine of RYGB-operated rats (0.50 ± 0.24 vs 0.17 ± 0.05 , ID%/mg), and lower FDG uptake in the liver (0.16 ± 0.03 vs 0.20 ± 0.02 , ID%/mg) and muscle (0.06 ± 0.02 vs 0.08 ± 0.01 , ID%/mg) compared with those of sham-operated rats (RYGB $n=8$, sham $n=5$). Right graph: Intestinal lumen phosphate buffered saline (PBS) washing analysis. Intestinal lumen PBS washings showed larger amount of FDG excretion in the RYGB rats (1.65 ± 2.05 vs 0.13 ± 0.11 , ID%, $p<0.001$). (G) Representative images of small intestinal FDG autoradiography of RYGB-operated and sham-operated rats after PBS lavage. Areas of higher FDG accumulation are darker in colour. (H) The graph shows the quantitative analysis of FDG uptake in the post-washing intestine tissue autoradiography images. RYGB-operated limbs showed higher FDG uptake in the alimentary limb (AL) and common limb (CL) compared with that in the corresponding sham intestine (AL: 0.36 ± 0.11 vs 0.22 ± 0.06 , $p=0.019$; CL: 0.41 ± 0.11 vs 0.19 ± 0.06 , $p=0.002$). (I, J) Representative three-dimensional (3D) reconstruction FDG PET/CT images showing changes in intestinal secretion before and after gastrectomy. (I) A 58-year-old man underwent gastrectomy for gastric cancer. The patient showed no change in hemoglobin A1c (HbA1c) or serum glucose level. Bowel glycolysis showed no significant change after gastrectomy. (J) A 69-year-old man underwent gastrectomy for gastric cancer. The HbA1c level decreased by 1.3% after gastrectomy, and serum glucose was reduced to 160 mg/dL. Compared with preoperative PET/CT, postoperative images showed that bowel glycolysis increased significantly after gastrectomy. 3D reconstruction images were generated using PMOD V.3.6 software (PMOD Technologies, Zürich, Switzerland). All data are presented as mean \pm SD, * $p<0.05$, ** $p<0.01$, *** $p<0.001$ versus sham.

that RYGB induced sustained weight loss and improved glycaemic control.

Altered CL AREG/EGFR/ GLUT1 signalling

To examine intestinal changes associated with whole-body metabolic improvements and increased FDG uptake in the CL, we compared the metabolic gene expression in selected regions of the CL with higher levels of FDG uptake (FDG [+]) or basal levels (FDG [–]) using RNA sequencing. Corresponding regions in sham-operated rats were included as additional controls. In accordance with previous findings,⁷ genes involved in glucose metabolism and cholesterol biosynthesis were upregulated in the AL and FDG (+) CL, but not in the BPL (online supplemental figure S2). Consistent with previous studies,^{8,9} we confirmed that genes upregulated in AL were upregulated in CL as well

(online supplemental figure S2). However, when we focused on the FDG uptake patterns (low FDG uptake in sham, low FDG uptake in AL, high FDG uptake in AL), we found a corresponding sequential increase in RNA gene expression patterns only in the CL, not in the AL (online supplemental figure S2). Based on the RNA-seq analysis, we assessed the pathway analysis and found that the gene sets related to the epidermal growth factor receptor (EGFR) signalling cascade were significantly upregulated (figure 2A). Of the EGFR ligands, only AREG showed a sequential increase in signalling correlating to FDG uptake increase patterns (sham ileum, CL FDG(–), CL FDG(+)). When we factored in FDG uptake patterns (low FDG uptake in sham, low FDG uptake in AL/CL, high FDG uptake in AL/CL), we found a sequential increase in RNA gene expression patterns only in the CL, and not in the AL (online supplemental figure

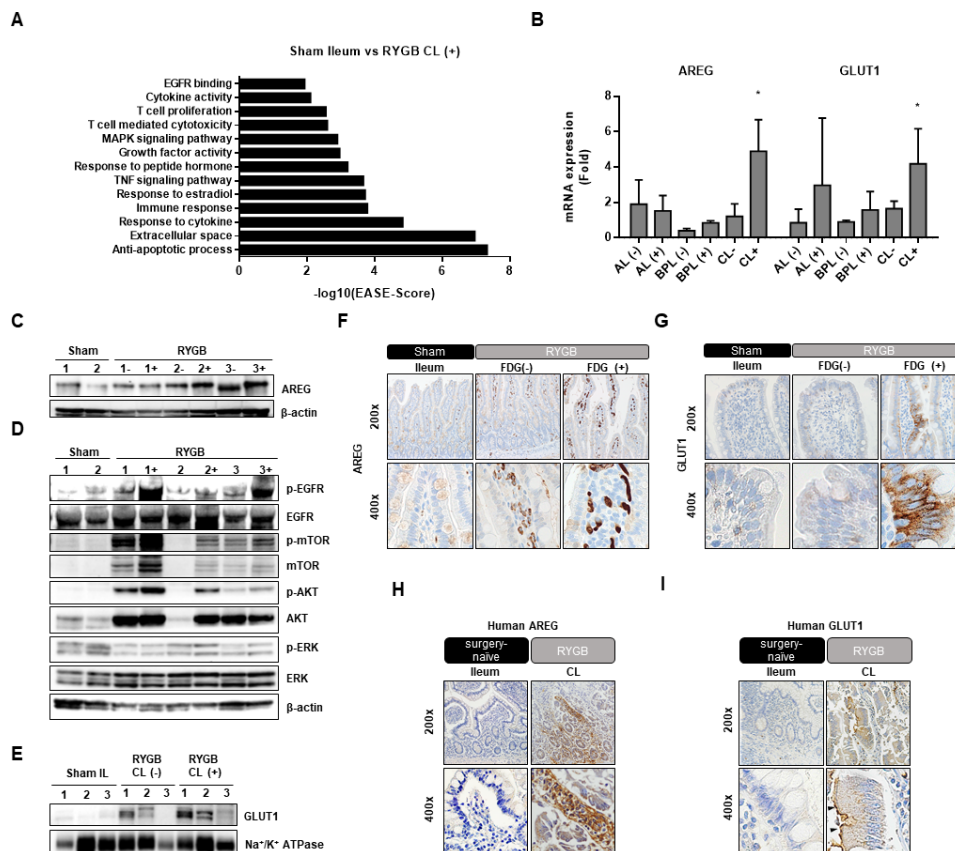


Figure 2 AREG/EGFR signalling is altered in Roux-en-Y gastric bypass (RYGB)-operated rats. (A) Pathway analysis of gene set enriched in the RYGB-operated common limb (CL) (+). (B) Expression of amphiregulin (AREG) and glucose transporter 1 (GLUT1) in the duodenum, jejunum and ileum of RYGB-operated rats and corresponding limbs of sham-operated rats. The fold change was calculated based on the corresponding sham-operated bowel (jejunum for the CL, duodenum for the biliopancreatic limbs (BPL) and ileum for the CL). (C) AREG protein expression in the ileum of RYGB-operated and sham-operated rats. Expression levels were normalised to that of β -actin. The number denotes the rat number and (-) or (+) denotes 2-deoxy-2-[18F]-fluoro-D-glucose (FDG) negativity or positivity of individual rats. (D) Immunoblots of the ileum obtained from sham-operated and RYGB-operated rats 4 weeks after surgery. Expression levels were normalised to that of the reference protein β -actin. The number denotes the rat number and (-) or (+) denotes FDG negativity or positivity of individual rats. (E) Surface proteins showing that endogenous GLUT1 increases its membrane (normalised against Na^+/K^+ ATPase) abundance in RYGB-operated rats 4 weeks after surgery. Representative images of AREG (F) and GLUT1 (G) immunostaining in the CL of RYGB-operated and the equivalent region of sham-operated rats 4 weeks postoperative. (H) Representative images of AREG (H) and GLUT1 (I) immunostaining in the human ileum of RYGB-operated and surgery-naïve patients. Data are presented as mean \pm SD (n=6). *p<0.05 versus (-) of each limb; **p<0.01 vs sham.

S3). This led us to target the CL. Therefore, we surmised that AREG is the dominant EGFR ligand that increases CL glucose metabolism (online supplemental figure S3).

Next, we analysed AREG expression in each limb of the RYGB-operated rats and the corresponding regions in the sham-operated rats. Based on reverse transcription PCR (RT-PCR) analysis, AREG expression was 4.9-fold higher in the FDG (+) CL of RYGB-operated rats than in that of sham rats, and was 4.0-fold higher than that in the FDG (-) CL of RYGB rats (figure 2B). Western blotting indicated that AREG protein levels were higher in the FDG (+) CL than in the FDG (-) CL and the ileum of sham rats (figure 2C, online supplemental figure S5), which was confirmed using IHC staining (figure 2F).

Furthermore, downstream signals of AREG and EGFR/mTOR/protein kinase B (AKT) pathways were more active in FDG (+) CL regions of RYGB-operated rats than in FDG (-) CL regions of RYGB-operated rats and the intestines of sham-operated rats, suggesting an increase in anabolic activity and increased glucose utilisation in FDG (+) regions following RYGB (figure 2D). We then evaluated membrane localised GLUT1 expression in the CL limb, and found that membrane-bound GLUT1 expression

was higher in RYGB-operated rats than in the sham-operated rats and was the highest in the FDG (+) CL (figure 2E). This pattern was also observed in IHC staining and RT-PCR for AREG and GLUT1, as progressively stronger staining was seen in the FDG (+) CL compared with that in the FDG (-) CL and sham-operated rats (figure 2B, F and G). Considering that AREG positive cells were identified in lamina propria of villi, which revealed a large number of lymphocytes in this site (data not shown), further IHC studies were performed. Cells positive for CD4 IHC staining in the lamina propria of villi colocalised with AREG and CD4 on immunofluorescence staining were identified. These results suggested that AREG correlated or originated from activated T helper 2 cells (online supplemental figure S4A, B).

These findings were confirmed using immunohistochemistry (IHC) staining of autopsy specimens obtained from the National Forensic Service. The staining for AREG was negative in the mucosa of surgery-naïve patients, but exhibited strong immunoreactivity in the blood vessel within the lamina propria of the ileal mucosa in RYGB-treated patients (figure 2H). In line with the findings in the animal studies, GLUT1 staining also

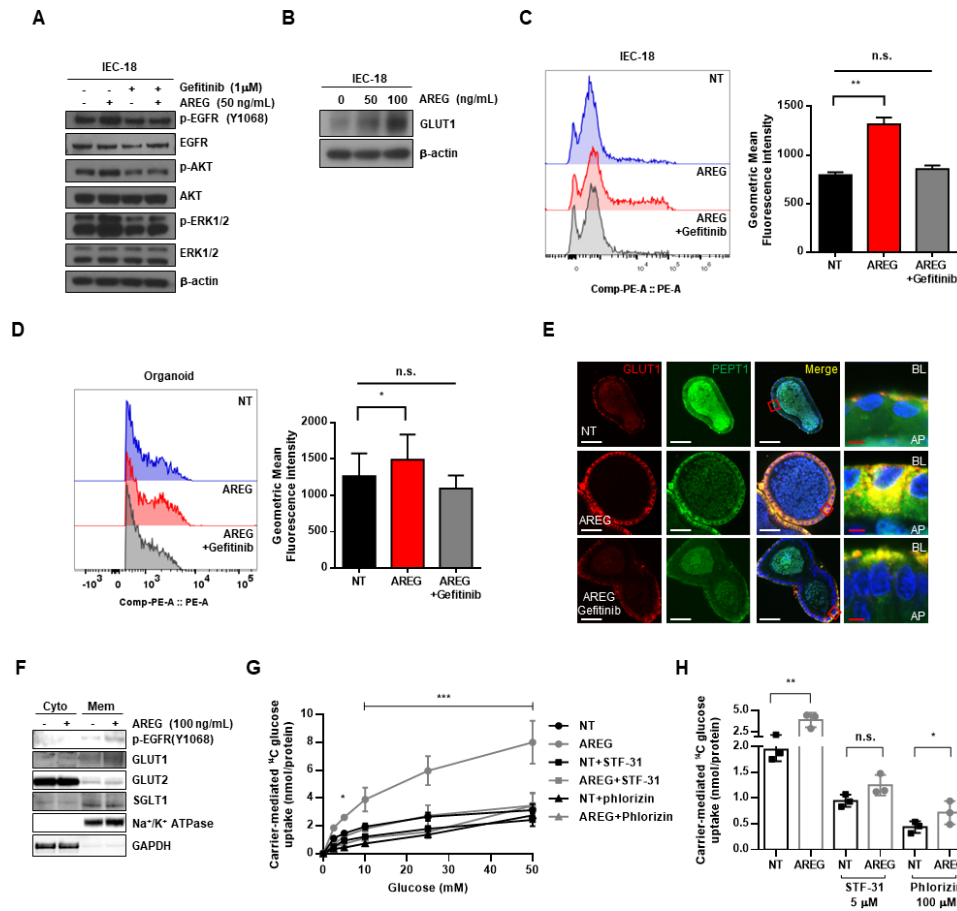


Figure 3 Amphiregulin (AREG) increases glucose uptake and secretion in an ileum cell line through EGFR-mediated glucose transporter 1 (GLUT1) expression and trafficking. (A) Immunoblots of IEC-18 cells treated with gefitinib (1 μ M), AREG (50 ng/mL) or both for 6 hours. Expression levels were normalised to that of β -actin. (B) Immunoblots of lysates of IEC-18 cells treated with 0, 50 or 100 ng/mL AREG for 24 hours. GLUT1 expression was normalised to that of β -actin. (C, D) Effect of AREG or AREG+Gefitinib treatment on membrane GLUT1 localisation in (C) IEC-18 cells and (D) organoids using flow cytometry. Left graph: representative images of the fluorescent labelling of GLUT1 on the cell surface. Right bar graph: GLUT1 localisation to the plasma membrane (unpaired t-test analysis). (E) Immunofluorescence staining of GLUT1 and PEPT-1 in untreated (NT) and AREG (100 ng/mL)-treated and gefitinib (1 μ M)-treated organoids. Immunofluorescence staining of GLUT1 (CY3, Red), PEPT-1 (FITC, green) and membrane colocalisation (merged, yellow). Basolateral side (BL) and apical side (AP). The white bar indicates 50 μ m and the red bar indicates 5 μ m. (F) Immunoblots of cytoplasm (Cyto) and plasma membrane (Mem) lysates of organoids. GAPDH served as a loading control of Cyto protein and Na⁺/K⁺ ATPase served as a loading control of Mem protein. (G) comparison of ¹⁴C-glucose uptake in AREG and non-treated (NT) IEC-18 cell lines. Higher glucose concentrations resulted in increased ¹⁴C-glucose uptake, with higher levels in AREG-treated cells compared with that in the NT cells. AREG-induced increased ¹⁴C-glucose uptake is mitigated after STF-31 administration (two-way analysis of variance (ANOVA), post hoc Tukey multiple comparison test). (H) Cross-sectional graph of ¹⁴C-glucose uptake in physiologically relevant high glucose concentrations (10 mM). Overall reduction of ¹⁴C-glucose uptake after STF-31 and phlorizin treatment in both AREG and NT IEC-18 cell lines. AREG-induced increased ¹⁴C-glucose uptake is mitigated after STF-31 administration, but in phlorizin treatment, AREG showed higher ¹⁴C-glucose uptake compared with NT (unpaired t-test). (All data are presented as mean \pm SD, ns, not significant, * p <0.05, ** p <0.01, *** p <0.001.)

revealed increased immunoreactivity in the cytoplasmic and luminal membrane in RYGB patients, whereas immunoreactivity was weak in surgery-naïve patients. (figure 2I). Together, these results showed that glucose excretion in rats and in humans in the CL may increase through activation of the AREG/EGFR/GLUT1 pathway after RYGB.

AREG enhances glucose uptake and secretion in polarised intestinal cells through EGFR/GLUT1 signalling

Next, we investigated whether exogenously administered AREG would induce GLUT1 expression and in turn regulate glucose uptake in IEC-18 normal ileal rat cells. On treatment with AREG, protein expression changes in IEC-18 cells were similar to those observed in the FDG (+) CL in vivo. AREG treatment-induced EGFR and AKT phosphorylation (figure 3A) and upregulated

GLUT1 in a dose-dependent manner (figure 3B). GLUT1 induction through EGFR signalling was prevented after treatment with the EGFR blocker, gefitinib (figure 3A). To evaluate the functional capacity of GLUT1, we performed flow cytometry analysis of surface GLUT1 staining. After AREG treatment, both mouse intestinal organoids and IEC-18 cells showed an increase in surface GLUT1 expression (IEC-18: 166 \pm 15.1% vs 100 \pm 6.8%; organoids: 118.1 \pm 5.7% vs 100.0%, figure 3C,D). AREG-induced GLUT1 upregulation and translocation were inhibited by gefitinib (IEC-18: AREG vs AREG+Gefitinib: 166 \pm 15.1% vs 107.9 \pm 8.2%; organoids: 118.1 \pm 5.7% vs 87 \pm 7.2%, figure 3C,D). Organoids were co-stained for PEPT1, an apical marker,¹⁰ to identify the apical membrane. In intestinal organoids treated with AREG, GLUT1 migrated to and colocalised with PEPT1 (figure 3E). Importantly, cytoplasmic GLUT1

migrated not only to the basolateral surface but also to the apical membrane (figure 3E). In AREG-treated intestinal organoids, the cytoplasmic and membrane proteins were separated, and GLUT1, GLUT2 and SGLT1 expression changes were evaluated using western blot and RT-qPCR. There were no significant changes in GLUT2 and SGLT1 expression levels; however, GLUT1 overexpression was observed in both the cytosol and the membrane (figure 3F). Real-time PCR also showed similar results, as only the GLUT1 expression level was increased after AREG treatment, and this effect was reduced after gefitinib treatment (online supplemental figure S6).

To evaluate the effect of AREG on glucose uptake, *in vitro* ^{14}C -glucose incubation studies were performed using various glucose concentrations. ^{14}C -glucose uptake was significantly higher in AREG-treated than in non-treated (NT) IEC-18 cells (figure 3G). This contribution of AREG to glucose uptake was offset when we incubated AREG cells with STF-1, a GLUT1-specific inhibitor (figure 3H). In contrast, treatment with the SGLT inhibitor phlorizin showed that AREG-treated cells had significantly higher amounts of glucose transported compared with that of NT cells (0.72 ± 0.23 vs 0.44 ± 0.11 , $p < 0.05$, figure 3H). These findings indicated that higher extracellular glucose concentrations result in GLUT1 membrane translocation; AREG-treated IEC-18 cells, exhibiting elevated intracellular GLUT1 expression, had a higher influx of glucose.

RYGB-induced hyperglycaemia improvement is reduced on local administration of GLUT1 inhibitor in the CL of the ileum

We evaluated the functional effect of GLUT1 upregulation on serum glucose normalisation after RYGB. The GLUT1

inhibitor STF-31 was locally administered into the CL of DIO rats during RYGB surgery using a hydrogel^{11 12} to continuously inhibit GLUT1 function (figure 4A). Eight days after surgery, the improvement in RYGB-induced hyperglycaemic was decreased in both GLUT1 inhibitor-treated and NT RYGB rats compared with that in sham-operated rats, with significantly lower improvement in glucose control in inhibitor-treated RYGB rats than in NT RYGB rats (figure 4B). Autoradiography revealed significantly lower FDG uptake in the CL of GLUT1 inhibitor-treated RYGB rats than in that of NT RYGB rats (figure 4C), which was confirmed using quantitative analysis (figure 4D). Together, these findings confirmed the pivotal role of GLUT1 as a conduit for serum glucose excretion into the intestinal lumen.

Exogenous supplementation of ileum-specific AREG mimics RYGB-mediated glycaemic control

To confirm the effects of AREG on glucose excretion from the serum into the small intestinal lumen, we delivered AREG locally into the ileum using hydrogel, which has been previously shown to release peptides in a sustained manner.¹² AREG-treated mice showed a bowel hypertrophy phenotype similar to that observed after bariatric surgery, with significant improvements in serum glucose levels (figure 5A,B). A two-way ANOVA was used to examine the effect of drugs (AREG) and time (pre-post) on OGTT changes. There was a significant interaction between the effects of drug and time on OGTT levels ($p = 0.0048$). Simple main effects analysis showed that both drug ($p = 0.0197$) and time ($p = 0.0008$) were significantly associated with AUC value. Importantly, we found that GLUT1 was upregulated in the intestines of AREG-treated mice (figure 5C and online supplemental

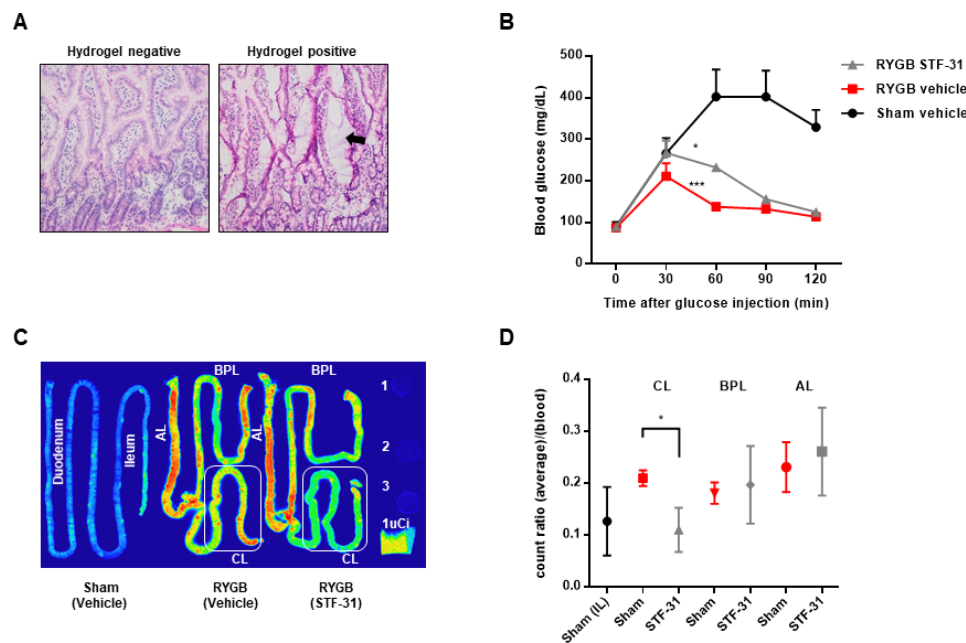


Figure 4 Blunted improvement of hyperglycaemia by local administration of glucose transporter 1 (GLUT1) inhibitor in the common limb (CL). (A) Representative H&E-stained slides of hydrogel retention in the common ileum (arrow) ($n = 4$). (B) Oral glucose tolerance test (OGTT) data for GLUT1 inhibitor (STF-31)-treated and vehicle-treated Roux-en-Y gastric bypass (RYGB)-operated and sham-operated rats. Both RYGB groups showed significant improvement in glucose tolerance compared with that in the sham+vehicle group. This improvement in glucose tolerance was significantly reduced in the RYGB+STF-31 group compared with that in the RYGB+vehicle group ($n = 4$, analysis of variance (ANOVA) two-stage step-up method of Benjamini, Krieger and Yekutieli for multiple comparison correction). (C) Post-washing 2-deoxy-2-[^{18}F]-fluoro-D-glucose (FDG) autoradiography of sham-operated, vehicle-treated and STF-31-treated RYGB bowel specimens. The white box denotes lower FDG in the STF-31-treated CL than that of the vehicle-treated CL. Numbers 1, 2, 3 on autoradiography denote FDG exposure from $100 \mu\text{L}$ of blood from each rat. (D) FDG autoradiography of the relative radiotracer amount in each surgical limb after washing. The STF-31-treated CL shows significantly lower FDG uptake than the vehicle-treated CL (unpaired t-test). The sham-operated ileum was used for comparison. All data are presented as mean \pm SD.

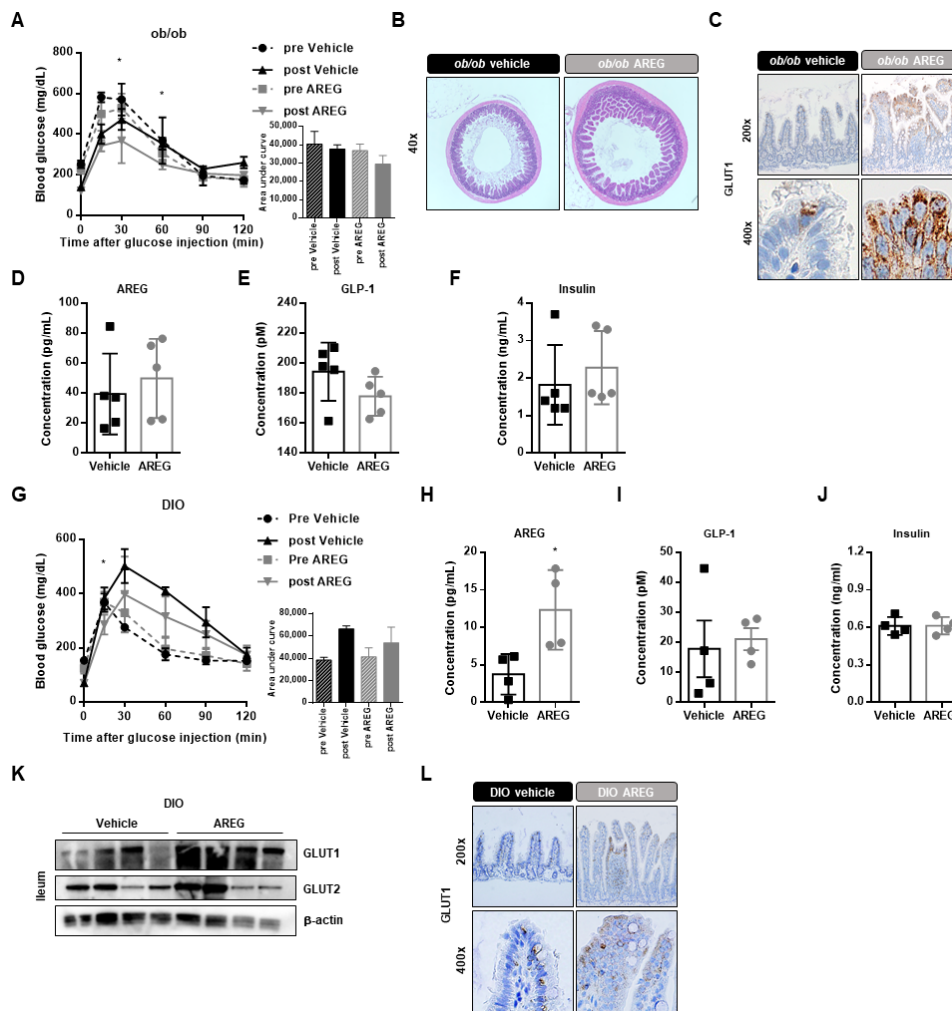


Figure 5 Ileum-localised or systemic amphiregulin (AREG) administration in vivo pharmacologically mimics Roux-en-Y gastric bypass (RYGB) glycaemic control. Ileum-localised treatment with vehicle or AREG (10 μ g) in *ob/ob* mice. (A) Oral glucose tolerance test (OGTT) of AREG-treated mice showed improvement in oral glucose tolerance ($n=5$). (B) H&E staining of the *ob/ob* mouse ileum. Note persistent intraluminal hydrogel after 1 week of administration. (C) GLUT1 immunostaining in the ileum of *ob/ob* mice transplanted with vehicle-containing or AREG-containing hydrogel. (D) serum AREG, (E) GLP-1, (F) and insulin concentrations at the time of sacrifice revealed no significant difference between vehicle-treated and AREG hydrogel-treated mice ($n=5$). (G) OGTT of vehicle-treated and AREG-treated (10 μ g, intraperitoneally injected) diet-induced obesity (DIO) mice. AREG-treated mice exhibited better glucose tolerance. (H) Serum AREG levels, (I) GLP-1 and (J) insulin concentrations in vehicle-treated and AREG-treated DIO mice ($n=4$). (K) Immunoblots of ileal lysates obtained from vehicle-treated or AREG-treated DIO mice. Expression levels were normalised to that of β -actin. (L) Representative images of GLUT1 immunostaining of the ileum and colon from vehicle-treated and AREG-treated DIO mice ($n=4$). * $p<0.05$; ** $p<0.01$; *** $p<0.001$.

figure S7). Locally administered AREG-treated mice did not exhibit significant changes in systemic concentrations of AREG, GLP-1 or insulin (figure 5D–F). We also confirmed that hydrogel treatment did not affect intestinal transit (online supplemental figure S8).

Lastly, experiments with systemic AREG-treated DIO mice confirmed these results. Similar to the results obtained with hydrogel, daily AREG administration (figure 5H) for 1 month improved hyperglycaemic and glucose intolerance (figure 5G) without significant changes in fasting serum GLP-1 and insulin levels (figure 5I, J). A two-way ANOVA was used to examine the effect of the drug (AREG) and time (pre-post) on OGTT. Simple main effects analysis showed that the drug ($p=0.0299$) was significantly associated with AUC; however, the time was not ($p=0.0737$). There was no significant interaction between the effects of drug and time on OGTT level ($p=0.3190$). AREG treatment significantly increased the expression of GLUT1 (vehicle:

1.00 ± 0.26 vs AREG: 1.65 ± 0.14) in the ileum, whereas GLUT2 expression showed no significant difference (vehicle: 1.0 ± 0.5 vs AREG: 1.76 ± 1.2 , figure 5K). Furthermore, IHC confirmed GLUT1 upregulation in the ileal epithelium of AREG-treated mice (figure 5L). Together, these results indicated that pharmacologically administered AREG can generate, at least in part, an RYGB surgery-like phenotype in surgery-naïve obese or diabetic rodent models via GLUT1 expression and sequestration.

DISCUSSION

This study revealed that in rats and humans, bariatric surgery resulted in AREG-stimulated EGFR-mediated GLUT1 overexpression in the CL intestinal epithelium, suggesting a novel mechanism underlying the excretion of serum glucose into the intestinal lumen. Previous studies reported changes in glucose-related transporters, including SGLT and GLUT, after surgery

or diabetes induction in mice.^{8 13–17} In particular, using FDG, Saeidi *et al*⁸ found that the intestine is a major glucose depository. We expanded on this hypothesis by demonstrating that AREG induction not only causes bowel hypertrophy, but also inadvertently causes serum glucose to excrete into the intestinal lumen via GLUT1.

Our results contribute to the existing literature on the role of glucose intestinal excretion in the context of RYGB and the potential clinical application of this mechanism in glucose control. We suggest that the intestinal growth phenotype stimulated from AREG activation (originating or contributed by T helper 2 cells) results in GLUT1 overexpression in the apical and basolateral membrane, possibly to provide enterocytes with the needed glucose for intestinal hypertrophy. However, as GLUT1 is a bilateral transporter, GLUT1 overexpression results in more serum glucose to reflux into the intestinal lumen, as the overall glucose gradient nearly always favours serum to lumen excretion¹⁸; hence, there is a need for an active transporter such as SGLT transporter to transport lumen glucose into the enterocyte.^{19 20} The overall dynamics of this glucose flux is captured in the autoradiograph analysis results, as the increased availability of glucose in the enterocytes is observed in the post-washing autoradiography, and the collected glucose (in the form of FDG or ¹⁴C-glucose) in the intestinal washings reveals the increased amount of serum glucose excreted into the intestinal lumen. Furthermore, the functional importance of GLUT1 overexpression in glucose control was shown (figure 4), as intraluminal GLUT1 inhibition in RYGB rats reduced the extent of RYGB-induced glucose homeostasis improvement.

Although our study is the first, to the best of our knowledge, to report serum glucose excretion into the intestinal lumen in RYGB rats and in patients, this phenomenon has been previously described in surgery-naïve rodents and humans.^{21–23} Regarding RYGB-induced changes, our results are in contrast to other studies,^{19 24} which have reported increased SGLT1 or GLUT in the AL after RYGB. We suggest that this discrepancy may be explained in that we used autoradiography to specifically pinpoint areas of increased glycolysis. Considering the heterogeneous glycolysis patterns and differential GLUT1 expression within the same limb, random sampling of the limb may result in the reported discrepancies.

It is well known that GLUT1 is induced through the activation of EGFR signalling in cancers and physiological processes.^{25–27} The growth phenotype induced by the EGFR pathway may have contributed to the increase in villous size and the formation of intestinal crypts in the rats after RYGB in this study (data not shown) and in other animal studies.^{8 13 28} Considering that AREG is involved in proliferative physiological functions, including intestinal tissue protection and repair, acute liver injury and regeneration, and fat metabolism,^{29 30} we hypothesised that AREG induction could be the initial physiological response to small intestinal shortening on bariatric surgery. This potentially explains why diabetes may recur a few years after bariatric surgery, as after the initial AREG-induced growth phenotype and subsequent glucose excretion into the intestinal lumen, once achieving sufficient intestinal mucosal growth, AREG expression may be ‘switched off’, causing glucose excretion into the lumen to cease.

Our results indicate that AREG is upregulated in areas of increased FDG uptake in the CL of RYGB rats and exogenous supplementation of AREG into surgery-naïve mice improves glucose homeostasis, although to a lesser extent, similar to RYGB surgery. Although EGFR is basolaterally located, local AREG administration should stimulate EGFR, as studies have

shown that breast milk contains EGF that stimulates intestine growth in newborns and in rodent studies.^{31–33}

Although we showed that AREG administration mimics RYGB-induced glucose homeostasis effects, AREG may be correlated with cancer,³⁴ and although the overall risk for cancer does not increase after bariatric surgery,^{35 36} further studies are needed to evaluate the safety of using AREG. Additionally, alternative targets should be evaluated, especially GLUT2, which has been reported in the apical membrane in diabetic mice, may also contribute to intestinal glucose excretion.³⁷ In addition, a more robust study isolating the contributions of each limb with glucose homeostasis improvement is needed, as other studies have shown that glucose metabolism is increased in the AL. Another limitation of our study is that we used human specimens and clinical data of patients who underwent RYGB gastrectomy and not bariatric surgery. Finally, assessing the correlation between glycaemia reduction and recovery of faecal ¹³C-glucose in post-RYGB patients would be helpful in evaluating the contribution of intestinal glucose excretion in glucose homeostasis against the known changes in systemic hormone levels and metabolism changes in multiple systemic organs.

In conclusion, this study revealed that AREG expression is induced in the CL after metabolic surgery, resulting in serum glucose excretion into the intestinal lumen via EGFR-mediated GLUT1 overexpression. This novel mechanism may partially account for rapid hyperglycaemic amelioration after metabolic surgery and potentially provides novel insights into the development of antidiabetic and weight loss medication.

Author affiliations

¹Department of Surgery, Gangnam Severance Hospital, Yonsei University College of Medicine, Seoul, Republic of Korea

²Brain Korea 21 PLUS Project for Medical Science, Yonsei University, Seoul, Republic of Korea

³Department of Forensic Medicine, Yonsei University College of Medicine, Seoul, Republic of Korea

⁴Endocrinology, Institute of Endocrine Research, Department of Internal Medicine, Yonsei University College of Medicine, Seoul, Republic of Korea

⁵Department of Medical Engineering, Yonsei University College of Medicine, Seoul, Republic of Korea

⁶Department of Nuclear Medicine, Yonsei University College of Medicine, Seoul, Republic of Korea

⁷Department of Surgery, Yonsei University College of Medicine, Seoul, Republic of Korea

⁸Department of Pathology, Gangnam Severance Hospital, Yonsei University College of Medicine, Seoul, Republic of Korea

Correction notice This article has been corrected since it published Online First. The email addresses for both corresponding authors have been corrected.

Acknowledgements We thank Byung Gon Kim and Jung-Hyun Ji, members of the laboratory animal research centre of ABMRC at Yonsei University College of Medicine, for the technical support with animal experiments. We also thank the Yonsei University College of Medicine statistics support team for statistical analysis and Editage (www.editage.co.kr) for English language editing.

Contributors Conceptualisation: CRK and AC. Data curation and formal analysis: CRK, CWK, IGK and AC. Funding acquisition: CRK. Investigation and methodology: CRK, CWK, EKW, TK, HJS, JPP, EJJ, WJH, SHN, IGK and AC. Supervision and validation: CRK, CWK and AC. Visualisation: CRK, CWK, JPP, YJL, JSS, JHO, NP, SS, MJ, WJK, IGK and AC. Writing original draft: CRK, CWK, IGK and AC. Writing review and editing: CRK, CWK, YJL, JSS, JHO, NP, IGK and AC.

Funding This research was supported by a grant from the Korea Health Technology R&D Project through the Korea Health Industry Development Institute (KHIDI), funded by the Ministry of Health & Welfare, Republic of Korea (grant number: HI18C1603).

Competing interests None declared.

Patient consent for publication Not required.

Ethics approval Approved by Severance Hospital’s institutional review board (4-2018-0595).

Provenance and peer review Not commissioned; externally peer reviewed.

Data availability statement Data are available upon reasonable request.

Supplemental material This content has been supplied by the author(s). It has not been vetted by BMJ Publishing Group Limited (BMJ) and may not have been peer-reviewed. Any opinions or recommendations discussed are solely those of the author(s) and are not endorsed by BMJ. BMJ disclaims all liability and responsibility arising from any reliance placed on the content. Where the content includes any translated material, BMJ does not warrant the accuracy and reliability of the translations (including but not limited to local regulations, clinical guidelines, terminology, drug names and drug dosages), and is not responsible for any error and/or omissions arising from translation and adaptation or otherwise.

ORCID iDs

In Gyu Kwon <http://orcid.org/0000-0002-1489-467X>
 Chan Woo Kang <http://orcid.org/0000-0001-5822-5235>
 Jong-Pil Park <http://orcid.org/0000-0002-6525-3012>
 Ju Hun Oh <http://orcid.org/0000-0003-0795-6649>
 Eun Kyung Wang <http://orcid.org/0000-0002-3243-3009>
 Tae Young Kim <http://orcid.org/0000-0002-6483-128X>
 Jin Sol Sung <http://orcid.org/0000-0002-7899-8814>
 Namhee Park <http://orcid.org/0000-0003-3135-9756>
 Yang Jong Lee <http://orcid.org/0000-0002-4620-5621>
 Hak-Joon Sung <http://orcid.org/0000-0003-2312-2484>
 Eun Jig Lee <http://orcid.org/0000-0003-3231-9887>
 Woo Jin Hyung <http://orcid.org/0000-0002-8593-9214>
 Su-Jin Shin <http://orcid.org/0000-0001-9114-8438>
 Sung Hoon Noh <http://orcid.org/0000-0003-4386-6886>
 Mijin Yun <http://orcid.org/0000-0002-1712-163X>
 Won Jun Kang <http://orcid.org/0000-0002-2107-8160>
 Arthur Cho <http://orcid.org/0000-0001-8670-2473>
 Cheol Ryong Ku <http://orcid.org/0000-0001-8693-9630>

REFERENCES

- Pories WJ, Caro JF, Flickinger EG, *et al.* The control of diabetes mellitus (NIDDM) in the morbidly obese with the Greenville gastric bypass. *Ann Surg* 1987;206:316–23.
- Pories WJ, MacDonald KG, Flickinger EG, *et al.* Is type II diabetes mellitus (NIDDM) a surgical disease? *Ann Surg* 1992;215:633–43.
- Schauer PR, Bhatt DL, Kirwan JP, *et al.* Bariatric surgery versus intensive medical therapy for diabetes--3-year outcomes. *N Engl J Med* 2014;370:2002–13.
- Pories WJ, Swanson MS, MacDonald KG, *et al.* Who would have thought it? an operation proves to be the most effective therapy for adult-onset diabetes mellitus. *Ann Surg* 1995;222:339–52.
- Ku CR, Lee N, Hong JW, *et al.* Intestinal glycolysis visualized by FDG PET/CT correlates with glucose decrement after gastrectomy. *Diabetes* 2017;66:385–91.
- Cho A, Kwon IG, Kim S, *et al.* Altered systematic glucose utilization after gastrectomy: correlation with weight loss. *Surg Obes Relat Dis* 2020;16:900–7.
- Ben-Zvi D, Meoli L, Abidi WM, *et al.* Time-Dependent molecular responses differ between gastric bypass and dieting but are conserved across species. *Cell Metab* 2018;28:310–23.
- Saeidi N, Meoli L, Nestoridi E, *et al.* Reprogramming of intestinal glucose metabolism and glycemic control in rats after gastric bypass. *Science* 2013;341:406–10.
- Flynn CR, Albaugh VL, Cai S, *et al.* Bile diversion to the distal small intestine has comparable metabolic benefits to bariatric surgery. *Nat Commun* 2015;6:7715.
- McNeill H, Ozawa M, Kemler R, *et al.* Novel function of the cell adhesion molecule uvomorulin as an inducer of cell surface polarity. *Cell* 1990;62:309–16.
- Wang X, Chun YW, Zhong L, *et al.* A temperature-sensitive, self-adhesive hydrogel to deliver iPSC-derived cardiomyocytes for heart repair. *Int J Cardiol* 2015;190:177–80.
- Zachman AL, Wang X, Tucker-Schwartz JM, *et al.* Uncoupling angiogenesis and inflammation in peripheral artery disease with therapeutic peptide-loaded microgels. *Biomaterials* 2014;35:9635–48.
- Cavin J-B, Couvelard A, Lebtahi R, *et al.* Differences in alimentary glucose absorption and intestinal disposal of blood glucose after Roux-en-Y gastric bypass vs sleeve gastrectomy. *Gastroenterology* 2016;150:454–64.
- Jurowich CF, Rikkala PR, Thalheimer A, *et al.* Duodenal-jejunal bypass improves glycemia and decreases SGLT1-mediated glucose absorption in rats with streptozotocin-induced type 2 diabetes. *Ann Surg* 2013;258:89–97.
- Troy S, Soty M, Ribeiro L, *et al.* Intestinal gluconeogenesis is a key factor for early metabolic changes after gastric bypass but not after gastric lap-band in mice. *Cell Metab* 2008;8:201–11.
- Burant CF, Flink S, DePaoli AM, *et al.* Small intestine hexose transport in experimental diabetes. increased transporter mRNA and protein expression in enterocytes. *J Clin Invest* 1994;93:578–85.
- Boyer S, Sharp PA, Debnam ES, *et al.* Streptozotocin diabetes and the expression of GLUT1 at the brush border and basolateral membranes of intestinal enterocytes. *FEBS Lett* 1996;396:218–22.
- Sabti S, Naftalin R K. A physiological basis for simulation of the alimentary limb condition after Roux-en-Y gastric bypass surgery 2019.
- Baud G, Raverdy V, Bonner C, *et al.* Sodium glucose transport modulation in type 2 diabetes and gastric bypass surgery. *Surg Obes Relat Dis* 2016;12:1206–12.
- Crane RK. Na⁺-dependent transport in the intestine and other animal tissues. *Fed Proc* 1965;24:1000–6.
- Axon AT, Creamer B. The exsorption characteristics of various sugars. *Gut* 1975;16:99–104.
- Cocco AE, Hendrix TR. The effect produced by phlorizin and hypertonic saline on sugar movement from blood to intestinal lumen. *Bull. Johns Hopk. Hosp* 1965;117:296–305.
- Boyd CA, Parsons DS. Movements of monosaccharides between blood and tissues of vascularly perfused small intestine. *J Physiol* 1979;287:371–91.
- Cavin J-B, Bado A, Le Gall M. Intestinal adaptations after bariatric surgery: consequences on glucose homeostasis. *Trends Endocrinol Metab* 2017;28:354–64.
- Lim S-O, Li C-W, Xia W, *et al.* Egfr signaling enhances aerobic glycolysis in triple-negative breast cancer cells to promote tumor growth and immune escape. *Cancer Res* 2016;76:1284–96.
- Makinoshima H, Takita M, Saruwatari K, *et al.* Signaling through the Phosphatidylinositol 3-Kinase (PI3K)/Mammalian Target of Rapamycin (mTOR) Axis Is Responsible for Aerobic Glycolysis mediated by Glucose Transporter in Epidermal Growth Factor Receptor (EGFR)-mutated Lung Adenocarcinoma. *J Biol Chem* 2015;290:17495–504.
- Smith JA, Stallons LJ, Schnellmann RG. Renal cortical hexokinase and pentose phosphate pathway activation through the EGFR/Akt signaling pathway in endotoxin-induced acute kidney injury. *Am J Physiol Renal Physiol* 2014;307:F435–44.
- Taqi E, Wallace LE, de Heuvel E, *et al.* The influence of nutrients, biliary-pancreatic secretions, and systemic trophic hormones on intestinal adaptation in a Roux-en-Y bypass model. *J Pediatr Surg* 2010;45:987–95.
- Berasain C, Avila MA. Amphiregulin. *Semin Cell Dev Biol* 2014;28:31–41.
- Yang B, Kumoto T, Arima T, *et al.* Transgenic mice specifically expressing amphiregulin in white adipose tissue showed less adipose tissue mass. *Genes Cells* 2018;23:136–45.
- Berseth CL. Enhancement of intestinal growth in neonatal rats by epidermal growth factor in milk. *Am J Physiol* 1987;253:G662–5.
- Jacobs DO, Evans DA, Mealy K, *et al.* Combined effects of glutamine and epidermal growth factor on the rat intestine. *Surgery* 1988;104:358–64.
- Wagner CL, Taylor SN, Johnson D. Host factors in amniotic fluid and breast milk that contribute to gut maturation. *Clin Rev Allergy Immunol* 2008;34:191–204.
- Busser B, Sancey L, Brambilla E, *et al.* The multiple roles of amphiregulin in human cancer. *Biochim Biophys Acta* 2011;1816:119–31.
- Almazeera S, El-Abd R, Al-Khamis A, *et al.* Role of bariatric surgery in reducing the risk of colorectal cancer: a meta-analysis. *Br J Surg* 2020;107:348–54.
- Schauer DP, Feigelson HS, Koebnick C, *et al.* Bariatric surgery and the risk of cancer in a large multisite cohort. *Ann Surg* 2019;269:95–101.
- Tobin V, Le Gall M, Fioramonti X, *et al.* Insulin internalizes GLUT2 in the enterocytes of healthy but not insulin-resistant mice. *Diabetes* 2008;57:555–62.